Title
Differential effects of risuteganib and bevacizumab on AMD cybrid cells

Authors
Schneider, Kevin
Chwa, Marilyn
Atilano, Shari R
et al.

Publication Date
2021-02-01

DOI
10.1016/j.exer.2020.108287

Peer reviewed

HHS Public Access

Author manuscript

Exp Eye Res. Author manuscript; available in PMC 2022 August 15.

Published in final edited form as:

Exp Eye Res. 2021 February ; 203: 108287. doi:10.1016/j.exer.2020.108287.

Differential effects of risuteganib and bevacizumab on AMD cybrid cells

Kevin Schneider[a], **Marilyn Chwa**[a], **Shari R. Atilano**[a], **Zixuan Shao**[b], **John Park**[b], **Hampar Karageozian**[b], **Vicken Karageozian**[b], **M. Cristina Kenney**[a,c,*]

[a]Gavin Herbert Eye Institute, University of California Irvine, Irvine, CA, USA

[b]Allegro Ophthalmics, LLC, San Juan Capistrano, CA, USA

[c]Department of Pathology and Laboratory Medicine, University of California Irvine, Irvine, CA, USA

Abstract

Purpose: Intravitreal injections of anti-vascular endothelial growth factor (VEGF) treatments are currently used to treat wet age-related macular degeneration (AMD), diabetic retinopathy, and macular edema. Chronic, repetitive treatments with anti-VEGF may have unintended consequences beyond the inhibition of angiogenesis. Most recently, clinical trials have been conducted with risuteganib (RSG, Luminate®), which is anti-angiogenic and has neuroprotective and anti-inflammatory properties. Mitochondrial damage and dysfunction play a major role in development of AMD. Transmitochondrial cybrids are cell lines established by fusing human retinal pigment epithelial (RPE) cells that are Rho0 (lacking mtDNA) with platelets isolated from AMD subjects or age-matched normal subjects. Cybrid cell lines have identical nuclei but mitochondria from different subjects, enabling investigation of the functional consequences of damaged AMD mitochondria. The present study compares the responses of AMD cybrids treated with bevacizumab (Bmab, Avastin®) versus risuteganib (RSG, Luminate®).

Methods: Cybrids were created by fusing mtDNA depleted ARPE-19 cells with platelets from AMD or age-matched normal patients. AMD (n = 5) and normal (n = 3) cybrids were treated for 48 h with or without 1x clinical dose of 1.25 mg/50 μl (25,000 μg/ml) of Bmab or 1.0 mg/50 μl

*Corresponding author. Gavin Herbert Eye Institute, Ophthalmology Research Laboratory, University of California Irvine, Hewitt Hall, Room 2028 843 Health Science Road, Irvine, CA, 92697, USA, mkenney@uci.edu (M.C. Kenney).

Contribution of authors

Kevin Schneider, designed experiments, performed assays, interpreted data, wrote manuscript; Marilyn Chwa, created AMD and Normal cybrids; Shari R. Atilano, performed qRT-PCR assays; Zixuan Shao, provided research and writing support; John Park, Hampar Karageozian, and Vicken Karageozian, provided research support and supply of peptides; Cristina Kenney, designed experiments, interpreted data, wrote manuscript.

Declaration of interests

Declaration of Interests: M. Cristina Kenney: Discovery Eye Foundation is a 501(c)3 that has supported her mitochondrial research. She serves as a Board Member for DEF. The terms of this arrangement have been reviewed and approved by the University of California, Irvine in accordance with its conflict of interest policies. M. Cristina Kenney Collaborations with Allegro Ophthalmics, LLC.

Declaration of Interests for Kevin Schneider, Marilyn Chwa, Shari R. Atilano: None.

Declaration of Interests for Zixuan Shao, John Park, Hampar Karageozian, and Vicken Karageozian: Above authors are employees of Allegro Ophthalmics, LLC.

Appendix A. Supplementary data

Supplementary data to this article can be found online at https://doi.org/10.1016/j.exer.2020.108287.

(20,000 μg/ml) of RSG. Cultures were analyzed for levels of cleaved caspase 3/7 and NucLight Rapid Red staining (IncuCyte® Live Cell Imager), mitochondrial membrane potential (ΔΨm, JC1 assay) or reactive oxygen species (ROS, H2DCFDA assay). Expression levels of genes related to the following pathways were analyzed with qRT-PCR: Apoptosis (*BAX, BCL2L13*, *CASP-3, −7, −9*) angiogenesis (*VEGFA, HIF1α, PDGF*); integrins (*ITGB-1, −3, −5*, *ITGA-3, −5, -V*); mitochondrial biogenesis (*PGC1α POLG*); oxidative stress (*SOD2, GPX3, NOX4*); inflammation (*IL-6, −18, −1β, IFN-β1*); and signaling (*P3KCA, PI3KR1*). Statistical analyses were performed using GraphPad Prism software.

Results: The untreated AMD cybrids had significantly higher levels of cleaved caspase 3/7 compared to the untreated normal cybrids. The Bmab-treated AMD cybrids showed elevated levels of cleaved caspase 3/7 compared to untreated AMD or RSG-treated AMD cybrids. The Bmab-treated cybrids had lower ΔΨm compared to untreated AMD or RSG-treated AMD cybrids. The ROS levels were not changed with Bmab or RSG treatment. Results showed that Bmab-treated cybrids had higher expression levels of inflammatory (*IL-6, IL1-β*), oxidative stress (*NOX4*) and angiogenesis (*VEGFA*) genes compared to untreated AMD, while RSG-treated cybrids had lower expression levels of apoptosis (*BAX*), angiogenesis (*VEGFA*) and integrin (*ITGB1*) genes.

Conclusions: These data suggest that the mechanism(s) of action of RSG, an integrin regulator, and Bmab, a recombinant monoclonal antibody, affect the AMD RPE cybrid cells differently, with the former having more anti-apoptosis properties, which may be desirable in treating degenerative ocular diseases.

Keywords

Risuteganib; Bevacizumab; Age-related macular degeneration; Cybrids

1. Introduction

Age-related macular degeneration (AMD) is the leading cause of vision loss among the elderly population in the Western world. This progressively degenerative retinal disease exists either as dry or wet (neovascular) form. Wet AMD is characterized by choroidal neovascularization beneath the macular region, leading to rapid loss of vision. Fortunately, wet AMD can be treated by intravitreal injections of anti-VEGF medications, with most patients experiencing favorable outcomes. Dry AMD involves progressive loss of the retinal pigment epithelial (RPE) cells and the overlying photoreceptors via the apoptosis pathway. Presently, there is no reliable treatment for dry AMD, which represents the majority of the AMD patient population. Therefore, anti-apoptotic protective therapies to preserve retinal cells would be a significant move forward for AMD subjects.

Recent studies have demonstrated that mitochondrial damage and dysfunction play a major role in development of AMD. Transmission electron microscopy (TEM) shows disrupted mitochondria in RPE cells of AMD subjects (Feher et al., 2006). The mitochondria from AMD retinas show high levels of mtDNA damage, loss of function, and altered proteomic profiles of critical mitochondrial proteins (Karunadharma et al., 2010; Mueller et al., 2012; Nicholls and Minczuk, 2014; Nordgaard et al., 2006). Targeting of mitochondria with

mitotrophic compounds show potential to stabilize and improve visual function in AMD patients (Feher et al., 2003, 2005).

Transmitochondrial cybrids are an excellent model to investigate the functional consequences of damaged AMD mitochondria in human RPE cells. The cybrid cell lines are established by fusing platelets (containing high levels of mitochondria but lacking nuclei) isolated from AMD subjects or age-matched normal subjects with human RPE cells that are Rho0 (lacking mtDNA). Therefore, all cell lines have identical nuclei but contain either AMD or normal mitochondria, which allow differences in characteristics to be attributed to the mitochondrial content (Kenney et al., 2013, 2014). Studies show that cybrids possessing AMD mitochondria have increased levels of cell death, apoptosis, autophagy, and are more susceptible to oxidative stressors (Nashine et al., 2016). A variety of drugs/nutraceutical agents have been shown to rescue the damage in AMD cybrids (Nashine et al., 2017, 2018, 2019a, 2019b).

Integrins are cell surface receptors that bind to extracellular matrices and mediate responses to cellular stress. Various integrins have been associated with vitreoretinal diseases, including αvβ3 integrin with wet AMD; αvβ5 integrin and αvβ3 with proliferative diabetic retinopathy (Friedlander et al., 1995, 1996); and α5β1 integrin, the principal fibronectin receptor, with proliferative vitreoretinopathy (Zahn et al., 2010). Integrins bind with vascular endothelial growth factor receptor 2 (VEGFR2), which is required for VEGFR2 activation, signaling and VEGF-induced angiogenesis (Byzova et al., 2000; Simons et al., 2016; West et al., 2012).

Risuteganib (RSG) (also known as Luminate® or ALG-1001, Allegro Ophthalmics, LLC, San Juan Capistrano, CA) is a synthetic, RGD-class peptide that is currently under investigation for multiple retinal diseases including dry AMD, wet AMD and diabetic macular edema (DME). Intravitreal injections of RSG have been shown to improve visual acuity of dry AMD, wet AMD and DME patients (Kaiser et al., 2013; Kaiser, 2019; Kuppermann, 2019). RSG suppresses levels of multiple integrin subunits including those associated with pro-angiogenic integrins: αvβ3, αvβ5, and α5β1 (Kaiser et al., 2013). Under induced oxidative stress conditions, RSG has shown cytoprotective properties in multiple retinal cell culture models (Beltran et al., 2018; Yang et al., 2019). Studies show that it can inhibit multiple pathogenic pathways, including inflammation, angiogenesis and cell death, making it a promising therapeutic agent for many retinal and non-retinal diseases.

Bevacizumab (Bmab) (Avastin®, Genentech, San Francisco, CA) is a recombinant monoclonal antibody that selectively binds and inhibits VEGF-A attachment to its cell surface receptors. In 2004, Bmab received FDA approval for metastatic colorectal cancer treatment but is used routinely to treat other cancers. Due to its beneficial effects against neovascularization, Bmab has been used off label to treat ocular neovascularization in AMD, diabetic retinopathy, DME and neovascular glaucoma. Studies report that anti-VEGF drugs, including Bmab, can decrease metabolism, reduce proliferation and/or alter expression of genes related to angiogenesis, apoptosis, inflammation and oxidative stress *in vitro* in a variety of cell types, including RPE cells, Müller cells, retinal ganglion cells and choroidal endothelial cells (Caceres-Del-Carpio et al., 2020; Guo et al., 2010; Klettner et al., 2010;

Spitzer et al., 2007). Yet, chronic intravitreal injections may be associated with increased development of geographic atrophic in AMD patients and macular ischemia associated with DME (Comparison of Age-related Macular Degeneration Treatments Trials Research et al., 2012; Grunwald, 1998; Manousaridis and Talks, 2012).

The present study evaluates the responses of AMD cybrids with damaged mitochondria to treatment with either Bmab or RSG. The levels of cell viability, apoptosis, mitochondrial membrane potential (ΔΨm), reactive oxygen species (ROS) production, and changes in gene expression associated with angiogenesis, mitochondrial biogenesis, oxidative stress, inflammation and signaling pathways were assessed. Compared with untreated AMD cybrids, Bmab-treated AMD cybrids showed elevated caspase 3/7, decreased ΔΨm, and an increase in inflammatory (*IL-6, IL1-β*), oxidative stress (*NOX4*) and angiogenesis (*VEGFA*) gene expression. RSG-treated AMD cybrids showed no increase in caspase 3/7, maintained normal levels of ΔΨm, and did demonstrated decreased apoptotic and angiogenic gene expression, with no increase in inflammatory and oxidative stress genes.

2. Materials and methods

2.1. Cybrid cell lines generation and culture conditions

Institutional review board approval was obtained from the University of California, Irvine (IRB #2003–3131). Peripheral blood from five AMD and three age-matched normal subjects (Table 1) was collected in sodium citrate tubes and a portion of the blood was used to isolate total DNA using the DNA extraction kit (PUREGENE, Qiagen, Valencia, CA). The isolated total DNA was used for determination of mitochondrial haplogroup. Using a series of centrifugation steps, platelets were isolated from the peripheral blood, suspended in Tris buffer saline (TBS) and then fused with ARPE-19 cells that were deficient in mtDNA (Rho*0*), as described previously to create cybrids (Chomyn, 1996; Nashine et al., 2016). Cybrids were cultured until confluent in DMEM-F12 media containing 10% dialyzed fetal bovine serum (FBS), 100 unit/ml penicillin, 100 μg/ml streptomycin, 2.5 μg/ml fungizone, 50 μg/ml gentamycin and 17.5 mM glucose (see Table 2).

All experiments used cybrid cells at passage 5. In order to avoid confusion due to mixing of different mtDNA haplogroups (Kenney et al., 2014), the AMD cybrids (n = 5) and Normal cybrids (n = 3) used in this study all possessed the H mtDNA haplogroups as determined by allelic discrimination. There was no statistical difference between the mean ages of the AMD and Normal groups; (AMD, 80.0 ± 2.39 and Normal, 74.0 ± 2.65, p = 0.1582).

The AMD and normal cybrids were treated for 48 h with 1x clinical dose of Bmab or RSG. The 1x clinical dose was defined as 50 μl injected into four mLs of vitreous: For Bmab, it is 1.25 mg/50 μl (25,000 μg/ml) and for RSG, it is 1.0 mg/50 μl (20,000 μg/ml).

2.2. IncuCyte® Live Cell Imager NucLight and caspase 3/7 assay

Analysis of cleaved caspase 3/7 was performed utilizing the IncuCyte® Live Cell Imager system (Sartorius, Essen Biosciences, Ann Arbor, MI). AMD and normal cybrids (10,000 cells/well) were plated in 96-well plates and allowed to attach overnight. Once attached, media were changed to media containing desired drug treatments. This media also contained

NucLight Rapid Red live-cell nuclear dye (1:500 dilution), as well as caspase 3/7 green live-cell dye (1:1000 dilution). At this time, cells were placed into the IncuCyte® Live Cell imager and images were taken every 2–4 h depending on the experiment. Images collected include brightfield, as well as both red and green channels. At the conclusion of the experiment, a variety of different metrics were analyzed, including generalized cellular stress (based on NucLight dye intensity), and caspase levels through measurement of cleaved caspase 3/7 signal. Analyses were performed by IncuCyte® S3 2019A software and analyzed through the GraphPad Prism programs.

Before performing our study, we chose to examine whether the IncuCyte® Live cell imaging system would be a suitable system for the measurement of cellular stress/apoptosis. In order to test this we exposed AMD cybrid cells to increasing concentrations of amyloid beta, a compound shown to induce cellular stress and apoptosis in our AMD cybrid cell system (Nashine et al., 2017). Cells were treated with 5 μM, 10 μM and 20 μM amyloid beta, stained with NucLight Rapid Red and caspase 3/7 green live cell dyes, and imaged every 4 h for 72 h 5 pictures are taken per well and samples were plated in triplicate.

While NucLight Rapid Red is utilized as a nuclear tracking dye, manufacturer protocols suggest that damaged or otherwise unhealthy cells will demonstrate an increased NucLight staining intensity. We observed increasing intensity of NucLight staining as amyloid beta concentration increased (5 μM = 1.4-fold increase, 10 μM = 2.46-fold increase, 20 μM = 3.81-fold increase) (S.I. Fig. 1a). Additionally, we saw an increase in caspase 3/7 overlap staining as amyloid beta concentration increased (5 μM = 4.29-fold increase, 10 μM = 12.87-fold increase, 20 μM = 34.8-fold increase (S.I. Fig. 1b). These results suggest that increases in both NucLight Rapid Red staining intensity, and Caspase 3/7 overlap staining are associated with cellular stress and apoptosis. For this reason, we consider Caspase 3/7 as a suitable measure of cellular apoptosis, and NucLight signal intensity as a secondary measure of general cellular health.

2.3. Mitochondrial membrane potential (ΔΨm) assay

AMD cybrids (10,000 cells/well) were plated on 96-well plates and incubated for 24 h. Cells were then treated with 1x Bmab or RSG for 48 h. At the conclusion of the treatment, JC-1 reagent (5,5′,6,6′-tetrachloro-1,1′,3,3′- tetraethylbenzimidazolylcarbocyanine iodide) (Biotium, Hayward, CA) was added to cultures for 15 min. Fluorescence was measured using a Gemini XPS Microplate Reader (Molecular Devices) for red (excitation 550 nm and emission 600 nm) and green (excitation 485 nm and emission 545 mm) wavelengths. Intact mitochondria with normal ΔΨm appeared red, while cells with decreased ΔΨm were in a green fluorescent state. Experiments were analyzed in quadruplicate. Representative JC-1 assay images were taken using the IncuCyte® Live Cell imager at 4× magnification after fluorescence was measured via plate reader.

2.4. Reactive oxygen/nitrogen species (ROS) assay

AMD cybrids were plated in 96-well plates (10,000 cells/well) in quadruplicate and incubated for 24 h. Cells were treated with 1x RSG or Bmab for 48 h. ROS levels were measured with fluorescent dye 2,7-dichlorodihydrofluorescin diacetate (H2DCFDA,

Invitrogen-Molecular Probes, Carlsbad, CA) on a fluorescence plate reader using 490 nm for emission and 520 nm for excitation wavelengths (Gemini XPS Microplate Reader, Molecular Devices, Sunnyvale, CA). Representative ROS assay images were taken using the IncuCyte® Live Cell imager at 4× magnification after fluorescence was measured via plate reader.

2.5. Isolation of RNA nd amplification of cDNA

RNA was isolated from AMD cybrids using the RNeasy Mini-Extraction kit (Qiagen, Valencia, CA), following the manufacturer's protocol. cDNA generated from 2 μg of individual RNA samples was used for qRT-PCR analyses using the QuantiTect Reverse Transcription Kit (Qiagen).

2.6. Quantitative real-time PCR (qRT-PCR) analyses

qRT-PCR was performed on individual samples using QuantiFast SYBR Green PCR Kits (Qiagen, Germantown, MD) on an Applied Biosystems ViiA 7 real time quantitative PCR detection system. Primers (QuantiTect Primer Assay, Qiagen or KiCqStart Primers, Sigma, St. Louis, MO) were used to analyze 25 different genes in a variety of pathways including apoptosis (*BAX, BCL2L13*), caspases (*CASP3, CASP7, CASP9*), angiogenesis (*VEGFA, HIF1a, PDGF*), integrins (*ITGB1, ITGB3, ITGB5, ITGA3, ITGA5, ITGAV*), mitochondrial biogenesis (*PGC1a, POLG*), oxidative stress (*SOD2, GPX3, NOX4*), inflammation (*IL-6, IL-1β, IFN-β1, IL-18*), and the PI3K pathway (*PI3KCA, PI3KR1*). Primers were standardized with the *HPRT1* or *HMBS* housekeeping genes. All analyses were performed in triplicate. The fold values were calculated using the 2^(−ΔΔCt) formula (Radonic et al., 2004).

2.7. Statistical analyses

Data were subjected to statistical analyses by nonparametric Mann-Whitney *U* test using GraphPad Prism (Version 5.0, La Jolla, CA). A P-value of ≤0.05 was considered statistically significant (* <0.05, ** <0.01, *** <0.001, NS representative of non-significance). Error bars in the graphs represent SEM (standard error of the mean).

3. Results

3.1. Bmab treatment reduced cellular health and increased cleaved caspase 3/7 levels in AMD cybrids

In order to examine the effects of Bmab and RSG on cellular health, cybrid cells were treated with the indicated drugs at 1x clinical doses for 48 h and the effects on cellular health and cleaved caspase 3/7 staining were measured. Increased levels of cleaved caspase 3/7 overlapping with nuclear staining are associated with apoptotic cells. First, we determined the baseline difference between untreated normal and AMD cybrids. AMD cybrids demonstrate an increase in both NucLight intensity of 55% and Caspase 3/7 staining of 58% (1.55-fold and 1.58-fold, respectively, $p < 0.001$) indicating decreased cell health and increased levels of basal apoptosis in AMD cybrids relative to normal cybrids (Fig. 1a and b). We then determined the effect of Bmab and RSG on both normal and AMD cybrids. Normal cybrids treated with Bmab and RSG demonstrated no significant changes in either

NucLight or caspase 3/7 levels. When AMD cybrids were treated with RSG, there was no significant change in either NucLight or caspase 3/7 levels compared to untreated AMD cybrids. AMD cybrids treated with Bmab showed a further increase in NucLight intensity of 374% compared with untreated AMD cybrids. (1.55 fold for AMD untreated and 5.29-fold for AMD Bmab, $p < 0.001$). AMD cybrids treated with Bmab also demonstrated an 81.6% increase in caspase 3/7 of levels compared to the untreated AMD cybrids. (1.58-fold for AMD untreated and 2.396-fold for AMD Bmab, $p < 0.001$) (Fig. 1a and b). Representative images demonstrate increased NucLight intensity and increased caspase 3/7 overlap count with Bmab treatment (Fig. 1c–f).

3.2. Bmab treatment decreased ΔΨm in AMD cybrids

Changes in ΔΨm are associated with early stages of cell apoptosis, due to the decoupling of the respiratory chain and release of cytochrome *c*. In order to test for any effects of Bmab and RSG on ΔΨm, we utilized the JC1 ΔΨm assay (Fig. 2). 48-hour treatment with 1x Bmab significantly decreased ΔΨm in AMD cybrids by 34.6% compared with untreated AMD cybrids (0.654-fold, $p < 0.001$). RSG had no significant effect on ΔΨm (0.9941-fold, $p = 0.9$).

3.3. RSG and Bmab had no detectable effect on ROS levels in AMD cybrids

Elevated levels of ROS can cause diminished cell health by oxidation of proteins and lipids and damages to nucleic acids. In order to examine changes in ROS levels and oxidative stress due to drug treatments, H2DCFDA assays were performed. Compared to untreated control, Bmab and RSG had no detectable effect on ROS levels in AMD cybrids (Fig. 3).

3.4. RSG and Bmab treatments influenced gene expression in pathways relating to apoptosis, angiogenesis, oxidative stress and inflammation

RSG decreased expression of the pro-apoptotic gene *BAX by 28%* (0.72-fold, $p = 0.0159$) Fig. 4a). Treatment with Bmab reduced *BAX* gene expression by 16%. (0.84-fold, $p = 0.015$). Expression of *BCL2L1*3 had a downward trend in both RSG and Bmab treated cells, but did not reach significance. Expression of *CASP-3, −7, −9* were not influenced by either treatment (Fig. 4a). When looking at genes associated with angiogenesis, RSG decreased gene expression of *VEGFA* by 20% (0.8-fold, $p = 0.0357$) while Bmab increased expression 27.2% (1.272-fold, $p = 0.0357$); *PDGF* and *HIF1a* were not influenced by either treatment (Fig. 4b). Looking at genes associated with oxidative stress, RSG had no effect on the genes tested while Bmab increased expression of *NOX4* by 35.5% (1.355-fold, $p = 0.0159$); *SOD2* and *GPX3* were not influenced by either treatment (Fig. 4c). Examining genes in the integrin pathway showed that RSG decreased expression of *ITGB1* by 13% (0.87-fold, $p = 0.0317$), which is an integrin gene associated with angiogenesis (Fig. 4d). When examining inflammatory genes, RSG treatment had no effect on expression of *IFN-β1, IL-1β, IL-6* or *IL-18*, while treatment with Bmab increased expression of *IL-6* 36% (1.36-fold, $p = 0.0303$), and *IL-1β* by 38.3% (1.383-fold, $p = 0.0381$). (Fig. 4e). Neither RSG nor Bmab influenced expression of *PI3KCA* or *PI3KR1* (Fig. 4f). Finally, there was no change in *PGC1a* or *POLG*, genes associated with mitochondrial biogenesis, under either treatment (Fig. 4g).

4. Discussion

Neovascularization is a major event associated with retinal diseases, including diabetic retinopathy, wet AMD, and retinal vascular occlusions. Current treatments include intravitreal injections of anti-VEGF drugs, which are successful in many cases but not in others. Recent studies have shown mixed results in that some anti-VEGF drugs can increase the size of geographic atrophy in some AMD patients (Grunwald et al., 2014; Martin et al., 2012) and may affect severity of macular ischemia in patients with diabetic macular edema (Manousaridis and Talks, 2012). In other cases, however, treatments with anti-VEGF drugs have shown no associations with changes in geographic atrophy (Gillies et al., 2020) or that rates in geographic atrophy were dependent on continuous or discontinuous use of anti-VEGF drugs (Chakravarthy et al., 2013). Due to the varied impact these existing medications can have, there could be benefits from exploring new drugs for the treatment of AMD.

In this study, we compared the response of AMD cybrids to Bmab, a commonly used anti-VEGF drug, and RSG, an investigational drug that regulates pro-angiogenic integrins and is currently in clinical trials for AMD and DME. Real-time analyses using the IncuCyte® instrument showed that compared to untreated AMD cybrids, the Bmab-treated AMD cybrids had an increase in activated caspase-3/7 levels and a decrease in $\Delta\Psi m$, events that have been associated with apoptosis. These findings are in agreement with Caceres-del-Carpio studies showing a decline in $\Delta\Psi m$ and upregulation of apoptosis genes in Bmab-treated human retinal Müller cells (MIO-M1) (Caceres-Del-Carpio et al., 2020). Malik also showed that ARPE-19 cells treated with 1x, 2x and 10x Bmab concentrations had a decrease in $\Delta\Psi m$ compared to untreated (Malik et al., 2014).

In contrast, when the AMD cybrids in our study were exposed to RSG, there was no change in caspase-3/7 or the $\Delta\Psi m$ levels, suggesting the RSG treatment did not induce early apoptotic changes in these cells. The RNA levels for genes related to mitochondrial biogenesis, *PGC1α* and *POLG*, were similar in untreated, RSG-treated and Bmab-treated cybrids, which supports that the drug effects do not involve increased mitochondrial numbers.

After 48 h of exposure, ROS levels were not elevated in the RSG-treated or Bmab-treated AMD cybrids compared to untreated cybrids. In cultured MIO-M1 cells, there was a 33% increase in ROS levels after treatment with Bmab (Caceres-Del-Carpio et al., 2020), suggesting that the Müller cell line was more sensitive to oxidative stress than the AMD cybrid cells. The transcription levels of the antioxidant enzymes *SOD2* and *GPX3* were unchanged after treatment with either RSG or Bmab. Interestingly, Bmab-treated AMD cybrids had elevated expression of *NOX4*, while the RSG-treated AMD cybrids did not, again demonstrating a difference between the two drugs. Using either NADH or NADPH as electron donors, the *NOX4* enzyme generates superoxides (Shiose et al., 2001). The H2DCFDA assay used in this study measures the downstream oxidative stress elements (hydrogen peroxides, peroxynitrates and hydroxyl groups) but not superoxides, which may be why the measured ROS levels were unchanged in spite of higher *NOX4* levels. It also suggests that superoxides generated by the elevated *NOX4* expression in Bmab treated

cultures were most likely eliminated – most likely via increased activity of antioxidant enzymes.

When transcription levels were evaluated, we found that RSG treatment lowered *VEGFA* expression levels while the Bmab-treated AMD cybrids showed higher expression of VEGFA compared to the untreated cybrids. Alidzanovic et al. reported that Bmab-treated cancer patients displayed higher plasma VEGF levels due to antibody interference with protein degradation and receptor-mediated endocytosis (Alidzanovic et al., 2016). However, they reported no upregulation of VEGF by Bmab in normal fibroblasts *in vitro*. In another study, Bmab-treatment altered the intracellular VEGF/VEGF-R signaling pathways and led to a paradoxical increase in proliferation of glioblastoma cells *in vitro* (Simon et al., 2014). AMD cybrids have damaged mitochondria (Nashine et al., 2016, 2017) and may response to the anti-VEGF antibody medications differently than normal, healthy cells. This would support the hypothesis that RSG may be a less perturbing treatment compared to antibody therapies. We acknowledge that there are limitations to the use of the ARPE-19 cell line as a model of RPE function. Studies have found that ARPE-19 cells show decreased expression of certain RPE cell markers and proteins associated with the formation of tight junctions as well as a hypersensitivity to VEGF action. However, it has also been suggested that these limitations, also somewhat resemble the aged eye and/or pathologic conditions. However due to these limitations, further studies should be performed with alternative cell lines in order to fully explore the effects of these drugs (Ablonczy et al., 2011).

When expression levels of inflammation genes were analyzed, there was no change in RSG-treated AMD cybrids compared to the untreated cultures. In contrast, Bmab-treatment increased expression of pro-inflammatory cytokines *IL6*, and *IL1β* compared to the untreated AMD cybrids. These cytokines are involved in the inflammatory response and apoptosis, which suggest monthly intravitreal injections of Bmab may contribute to the inflammation associated with diabetic retinopathy and/or retinal cell damage seen in development of geographic atrophy in wet AMD patients. In diabetic patients, the protein levels of IL-6, IL-8 and TGF-β2 levels were significantly elevated after intravitreal injections of Bmab (Forooghian et al., 2010; Jeon and Lee, 2012). Future experiments analyzing the protein levels of pro-inflammatory cytokines would provide further evidence regarding the differences between RSG and Bmab treatments in our cybrid cell culture system. Our findings suggest that exposure to a small peptide, such as RSG, rather than an antibody fragment, may elicit less inflammatory response in the cellular environment.

The AMD cybrids treated with RSG demonstrated down-regulation of *ITGB1*, an integrin subunit that was elevated in both neovascular AMD and diabetic retinopathy as the α5β1 isoform (Gonzalez-Salinas et al., 2018; Gonzalez, 2016). The integrin expression levels were not altered when cells were exposed to Bmab, which is not surprising since it is a humanized monoclonal antibody, which would not be expected to modulate integrin levels. Lugano and coworkers reported that β1 integrin signaling is critical for fibronectin fibrillogenesis (Lugano et al., 2018). Loss of α5β1 integrin and fibronectin coincide with maturation of vessels along with upregulation of laminin and its receptors, α1β1 and α6β1 integrins (Milner and Campbell, 2002). Studies investigating RGD (arginine-glycine-aspartate) based

therapeutics to inhibit angiogenesis have been underway for treatments in cancers, ocular and systemic diseases (Gonzalez-Salinas et al., 2018; Gonzalez, 2016; Li et al., 2016).

In summary, RSG decreases pro-apoptotic gene expression (*BAX*), along with lowering *ITGB1* and *VEGFA* levels in the AMD cybrids compared to untreated cultures (Fig. 5). In contrast, the Bmab-treated AMD cybrids showed elevated levels of the pro-oxidative stress *NOX4*, pro-inflammatory genes (*IL-1β*, *IL-6*) and *VEGFA* compared to untreated cybrids. These data suggest that the mechanism(s) of action of RSG, an integrin regulator, and Bmab, a recombinant monoclonal antibody, affect the AMD RPE cybrid cells differently, with the former having more anti-apoptosis properties, which may be desirable in treating degenerative ocular diseases (Fig. 6).

Supplementary Material

Refer to Web version on PubMed Central for supplementary material.

Acknowledgements

We wish to thank the subjects who participated in this study. This work was supported by the Arnold and Mabel Beckman Foundation, Discovery Eye Foundation, Polly and Michael Smith, Edith and Roy Carver, and NEI R01 EY0127363 (MCK). Supported in part by an Unrestricted Departmental Grant from Research to Prevent Blindness. We acknowledge the support of the Institute for Clinical and Translational Science (ICTS) at University of California Irvine.

References

Ablonczy Z, Dahrouj M, Tang PH, et al. , 2011. Human retinal pigment epithelium cells as functional models for the RPE in vivo. Invest. Ophthalmol. Vis. Sci. 52 (12), 8614–8620. [PubMed: 21960553]

Alidzanovic L, Starlinger P, Schauer D, et al. , 2016. The VEGF rise in blood of bevacizumab patients is not based on tumor escape but a host-blockade of VEGF clearance. Oncotarget 7, 57197–57212. [PubMed: 27527865]

Beltran MZ-A, Gonzalez-Salinas R, Gulias-Cañizo R, et al. , 2018. Cytoprotective effect of ALG-1001 peptide (Luminate) on human retinal pigment epithelial cells exposed to oxidative injury. A novel functional-outcome for an Anti-VEGF agent. Invest. Ophthalmol. Vis. Sci. 59 (9), 1465.

Byzova TV, Goldman CK, Pampori N, et al. , 2000. A mechanism for modulation of cellular responses to VEGF: activation of the integrins. Mol. Cell 6, 851–860. [PubMed: 11090623]

Caceres-Del-Carpio J, Moustafa MT, Toledo-Corral J, et al. , 2020. In vitro response and gene expression of human retinal Muller cells treated with different anti-VEGF drugs. Exp. Eye Res. 191, 107903. [PubMed: 31904361]

Chakravarthy U, Harding SP, Rogers CA, et al. , 2013. Alternative treatments to inhibit VEGF in age-related choroidal neovascularisation: 2-year findings of the IVAN randomised controlled trial. Lancet 382 (9900), 1258–1267. [PubMed: 23870813]

Chomyn A, 1996. Platelet-mediated Transformation of Human Mitochondrial DNA-Less Cells. Academic Press, Inc., Salt Lake City, UT.

Comparison of Age-related Macular Degeneration Treatments Trials Research G, Martin DF, Maguire MG, et al. , 2012. Ranibizumab and bevacizumab for treatment of neovascular age-related macular degeneration: two-year results. Ophthalmology 119, 1388–1398. [PubMed: 22555112]

Feher J, Kovacs B, Kovacs I, et al. , 2005. Improvement of visual functions and fundus alterations in early age-related macular degeneration treated with a combination of acetyl-L-carnitine, n-3 fatty acids, and coenzyme Q10. Ophthalmologica 219, 154–166. [PubMed: 15947501]

Feher J, Kovacs I, Artico M, et al. , 2006. Mitochondrial alterations of retinal pigment epithelium in age-related macular degeneration. Neurobiol. Aging 27, 983–993. [PubMed: 15979212]

Feher J, Papale A, Mannino G, et al. , 2003. Mitotropic compounds for the treatment of age-related macular degeneration. The metabolic approach and a pilot study. Ophthalmologica 217, 351–357. [PubMed: 12913326]

Forooghian F, Kertes PJ, Eng KT, et al. , 2010. Alterations in the intraocular cytokine milieu after intravitreal bevacizumab. Invest. Ophthalmol. Vis. Sci. 51, 2388–2392. [PubMed: 20007836]

Friedlander M, Brooks PC, Shaffer RW, et al. , 1995. Definition of two angiogenic pathways by distinct alpha v integrins. Science 270, 1500–1502. [PubMed: 7491498]

Friedlander M, Theesfeld CL, Sugita M, et al. , 1996. Involvement of integrins alpha v beta 3 and alpha v beta 5 in ocular neovascular diseases. Proc. Natl. Acad. Sci. U. S. A. 93, 9764–9769. [PubMed: 8790405]

Gillies MC, Hunyor AP, Arnold JJ, et al. , 2020. Macular atrophy in neovascular age-related macular degeneration: a randomized clinical trial comparing ranibizumab and aflibercept (RIVAL study). Ophthalmology 127 (2), 198–210. [PubMed: 31619357]

Gonzalez-Salinas R, Hernandez-Zimbron LF, Gulias-Canizo R, et al. , 2018. Current anti-integrin therapy for ocular disease. Semin. Ophthalmol. 33, 634–642. [PubMed: 29087767]

Gonzalez V, 2016. The promise of integrin receptors for treating vitreoretinal disorders. Retina Today 76–78.

Grunwald JE, 1998. Vascular endothelial growth factor and severity of nonproliferative diabetic retinopathy mediate retinal hemodynamics in vivo: a potential role for vascular endothelial growth factor in the progression of nonproliferative diabetic retinopathy [letter; comment]. Am. J. Ophthalmol. 125, 731–732. [PubMed: 9625570]

Grunwald JE, Daniel E, Huang J, et al. , 2014. Risk of geographic atrophy in the comparison of age-related macular degeneration treatments trials. Ophthalmology 121, 150–161. [PubMed: 24084496]

Guo B, Wang Y, Hui Y, et al. , 2010. Effects of anti-VEGF agents on rat retinal Muller glial cells. Mol. Vis. 16, 793–799. [PubMed: 20454698]

Jeon S, Lee WK, 2012. Intravitreal bevacizumab increases intraocular interleukin-6 levels at 1 day after injection in patients with proliferative diabetic retinopathy. Cytokine 60, 535–539. [PubMed: 22846147]

Kaiser P, 2019. Safety and efficacy of Risuteganib in intermediate non-exudative age-related macular degeneration - first time results from a Phase 2 study. American Society of Retina Specialists Annual Meeting, Chicago. https://www.modernretina.com/article/asrs-2019-street-team-peter-k-kaiser-md.

Kaiser P, Boyer D, Campochiaro P, et al. , 2013. Integrin Peptide Therapy: the first wet AMD experience. Invest. Ophthalmol. Vis. Sci. 54, 2177.

Karunadharma PP, Nordgaard CL, Olsen TW, et al. , 2010. Mitochondrial DNA damage as a potential mechanism for age-related macular degeneration. Invest. Ophthalmol. Vis. Sci. 51, 5470–5479. [PubMed: 20505194]

Kenney MC, Chwa M, Atilano SR, et al. , 2014. Inherited mitochondrial DNA variants can affect complement, inflammation, and apoptosis pathways: insights into mitochondrial-nuclear interactions. Hum. Mol. Genet.

Kenney MC, Chwa M, Atilano SR, et al. , 2013. Mitochondrial DNA variants mediate energy production and expression levels for CFH, C3 and EFEMP1 genes: implications for age-related macular degeneration. PLoS One 8, e54339. [PubMed: 23365660]

Klettner A, Mohle F, Roider J, 2010. Intracellular bevacizumab reduces phagocytotic uptake in RPE cells. Graefes Arch. Clin. Exp. Ophthalmol. 248, 819–824. [PubMed: 20169356]

Kuppermann BD, 2019. Risuteganib for intermediate dry-AMD. Retin. Physician. https://www.retinalphysician.com/issues/2019/november-2019/risuteganib-for-intermediate-dry-amd.

Li Y, Li L, Li Z, et al. , 2016. Tat PTD-Endostatin-RGD: a novel protein with anti-angiogenesis effect in retina via eye drops. Biochim. Biophys. Acta 1860, 2137–2147. [PubMed: 27233450]

Lugano R, Vemuri K, Yu D, et al. , 2018. CD93 promotes beta1 integrin activation and fibronectin fibrillogenesis during tumor angiogenesis. J. Clin. Invest. 128, 3280–3297. [PubMed: 29763414]

Malik D, Tarek M, Caceres Del Carpio J, et al. , 2014. Safety profiles of anti-VEGF drugs: bevacizumab, ranibizumab, aflibercept and ziv-aflibercept on human retinal pigment epithelium cells in culture. Br. J. Ophthalmol. 98 (Suppl. 1), i11–i16. [PubMed: 24836865]

Manousaridis K, Talks J, 2012. Macular ischaemia: a contraindication for anti-VEGF treatment in retinal vascular disease? Br. J. Ophthalmol. 96, 179–184. [PubMed: 22250209]

Martin DF, Maguire MG, Fine SL, et al. , 2012. Comparison of Age-related Macular Degeneration Treatments Trials Research, G. Ranibizumab and bevacizumab for treatment of neovascular age-related macular degeneration: two-year results. Ophthalmology 119, 1388–1398. [PubMed: 22555112]

Milner R, Campbell IL, 2002. Developmental regulation of beta1 integrins during angiogenesis in the central nervous system. Mol. Cell. Neurosci. 20, 616–626. [PubMed: 12213443]

Mueller EE, Schaier E, Brunner SM, et al. , 2012. Mitochondrial haplogroups and control region polymorphisms in age-related macular degeneration: a case-control study. PLoS One 7, e30874. [PubMed: 22348027]

Nashine S, Chwa M, Kazemian M, et al. , 2016. Differential expression of complement markers in normal and AMD transmitochondrial cybrids. PLoS One 11, e0159828. [PubMed: 27486856]

Nashine S, Cohen P, Chwa M, et al. , 2017. Humanin G (HNG) protects age-related macular degeneration (AMD) transmitochondrial ARPE-19 cybrids from mitochondrial and cellular damage. Cell Death Dis. 8, e2951. [PubMed: 28726777]

Nashine S, Cohen P, Nesburn AB, et al. , 2018. Characterizing the protective effects of SHLP2, a mitochondrial-derived peptide, in macular degeneration. Sci. Rep. 8, 15175. [PubMed: 30310092]

Nashine S, Kanodia R, Nesburn AB, et al. , 2019a. Nutraceutical effects of Emblica officinalis in age-related macular degeneration. Aging 11, 1177–1188. [PubMed: 30792375]

Nashine S, Subramaniam SR, Chwa M, et al. , 2019b. PU-91 drug rescues human age-related macular degeneration RPE cells; implications for AMD therapeutics. Aging 11, 6691–6713. [PubMed: 31477635]

Nicholls TJ, Minczuk M, 2014. In D-loop: 40 years of mitochondrial 7S DNA. Exp. Gerontol. 56, 175–181. [PubMed: 24709344]

Nordgaard CL, Berg KM, Kapphahn, et al. , 2006. Proteomics of the retinal pigment epithelium reveals altered protein expression at progressive stages of age-related macular degeneration. Invest. Ophthalmol. Vis. Sci. 47, 815–822. [PubMed: 16505012]

Radonic A, Thulke S, Nitsche A, et al. , 2004. Guideline to reference gene selection for quantitative real-time PCR. Biochem. Biophys. Res. Commun. 313 (4), 856–862. [PubMed: 14706621]

Shiose A, Kuroda J, Tsuruya K, et al. , 2001. A novel superoxide-producing NAD(P)H oxidase in kidney. J. Biol. Chem. 276, 1417–1423. [PubMed: 11032835]

Simon T, Coquerel B, Petit A, et al. , 2014. Direct effect of bevacizumab on glioblastoma cell lines in vitro. NeuroMolecular Med. 16, 752–771. [PubMed: 25113866]

Simons M, Gordon E, Claesson-Welsh L, 2016. Mechanisms and regulation of endothelial VEGF receptor signalling. Nat. Rev. Mol. Cell Biol. 17, 611–625. [PubMed: 27461391]

Spitzer MS, Yoeruek E, Sierra A, et al. , 2007. Comparative antiproliferative and cytotoxic profile of bevacizumab (Avastin), pegaptanib (Macugen) and ranibizumab (Lucentis) on different ocular cells. Graefes Arch. Clin. Exp. Ophthalmol. 245, 1837–1842. [PubMed: 17347807]

West XZ, Meller N, Malinin NL, et al. , 2012. Integrin beta 3 crosstalk with VEGFR accommodating tyrosine phosphorylation as a regulatory switch. PLoS One 7, e31071. [PubMed: 22363548]

Yang P, Neal SE, Jaffe GJ, 2019. Luminate protects against hydroquinone–induced injury in human RPE cells. Invest. Ophthalmol. Vis. Sci. 60 (9), 1944.

Zahn G, Volk K, Lewis GP, et al. , 2010. Assessment of the integrin alpha5beta1 antagonist JSM6427 in proliferative vitreoretinopathy using in vitro assays and a rabbit model of retinal detachment. Invest. Ophthalmol. Vis. Sci. 51, 1028–1035. [PubMed: 19815730]

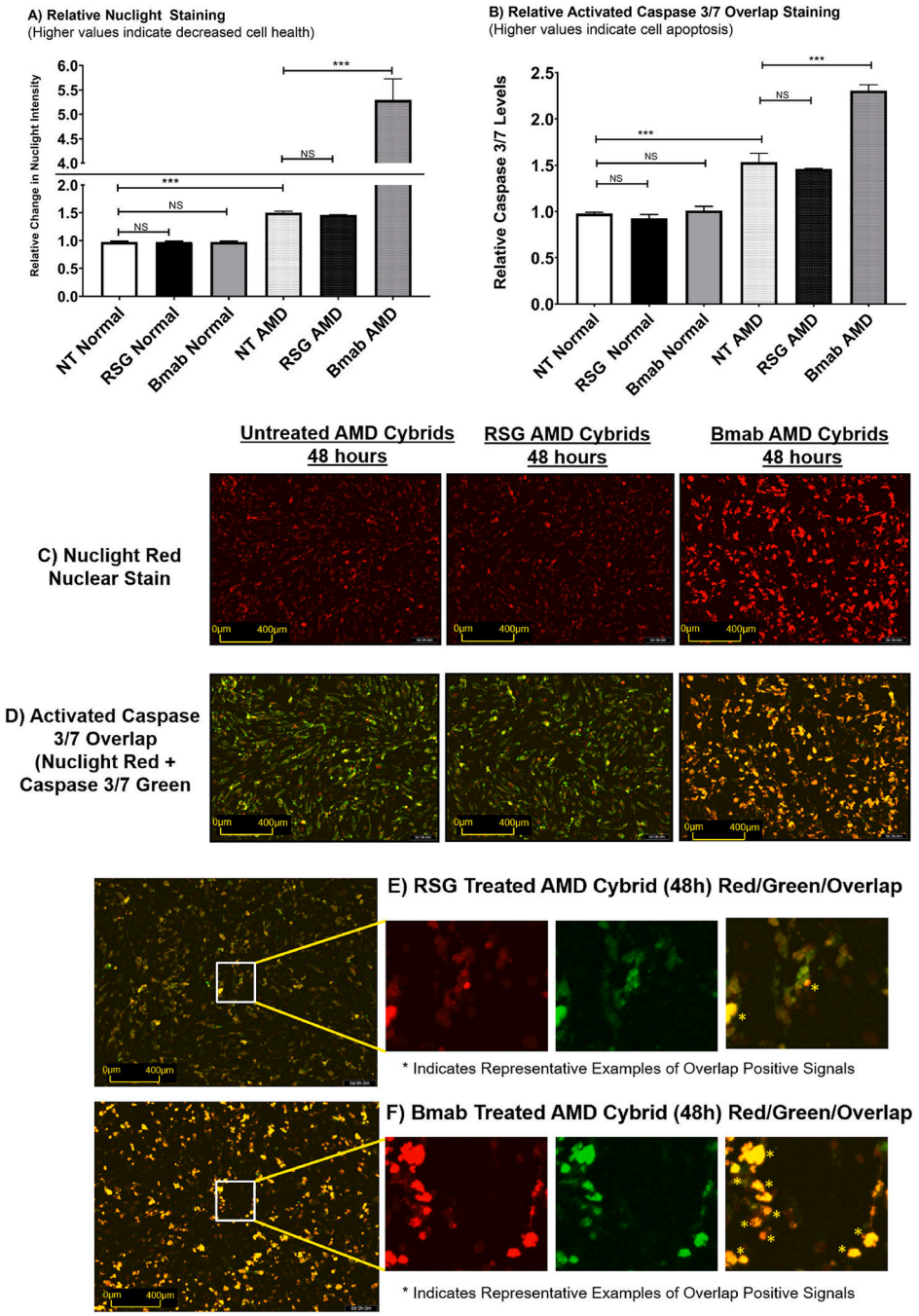

Fig. 1. Cell Health/Caspase Staining of Cybrids Treated with RSG and Bmab.

(A) Untreated AMD cybrids exhibit increased NucLight intensity by 55% (1.55-fold, $p < 0.005$) compared with normal cybrids. Normal cybrids treated with Bmab and RSG demonstrated no significant changes in NucLight intensity. When AMD cybrids were treated with RSG, there was no significant change in NucLight intensity. However, AMD cybrids treated with Bmab showed a further increase in NucLight intensity of 374%. (1.55-fold for untreated AMD and 5.29-fold for Bmab treated, $p < 0.001$. **(B)** Untreated AMD cybrids exhibit increased caspase 3/7 overlap staining by 58% (1.58-fold, $p < 0.005$) compared with

normal cybrids. Normal cybrids treated with Bmab and RSG demonstrated no significant changes in caspase 3/7 levels. When AMD cybrids were treated with RSG, there was no significant change in caspase 3/7 levels, while AMD cybrids treated with Bmab showed a further increase in caspase 3/7 levels compared to the normal cybrids. (1.58-fold for untreated AMD and 2.396-fold for Bmab treated AMD, $p < 0.001$). **(C)** Representative images of NucLight intensity in untreated, RSG- and Bmab-treated AMD cybrids at 48 h. **(D)** Representative images of caspase 3/7 overlap staining in untreated, RSG- and Bmab-treated AMD cybrids at 48 h. **(E–F)** High magnification images of NucLight, caspase 3/7, and overlap in RSG- and Bmab-treated AMD cybrids. Cells labeled with (*) are indicative of overlap positive signals. AMD cybrids (n = 5) and Normal cybrids (n = 3) Data were subjected to statistical analyses by nonparametric Mann-Whitney *U* test using GraphPad Prism (Version 5.0, La Jolla, CA). A P-value of ≤0.05 was considered statistically significant (* <0.05, ** <0.01, *** <0.001, NS representative of non-significance). Error bars in the graphs represent SEM (standard error of the mean).

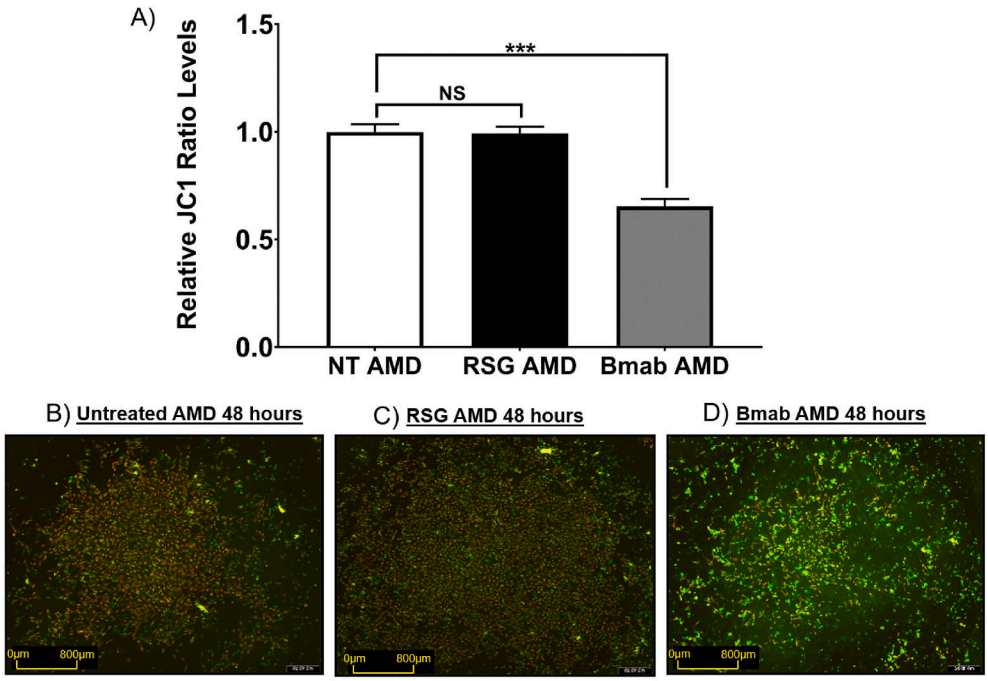

Fig. 2. Bmab treatment decreased ΔΨm in AMD cybrids.

(A) Bmab significantly decreased ΔΨm in AMD cybrids by 34.6% (0.654-fold, $p < 0.001$). RSG had no significant effect on ΔΨm (0.9941-fold, $p = 0.9$). **(B–D)** Representative JC1 fluorescence images from untreated, RSG- and Bmab-treated AMD cybrid cells. AMD cybrids (n = 5) Data were subjected to statistical analyses by nonparametric Mann-Whitney *U* test using GraphPad Prism (Version 5.0, La Jolla, CA). A P-value of ≤0.05 was considered statistically significant (* <0.05, ** <0.01, *** <0.001, NS representative of non-significance). Error bars in the graphs represent SEM (standard error of the mean).

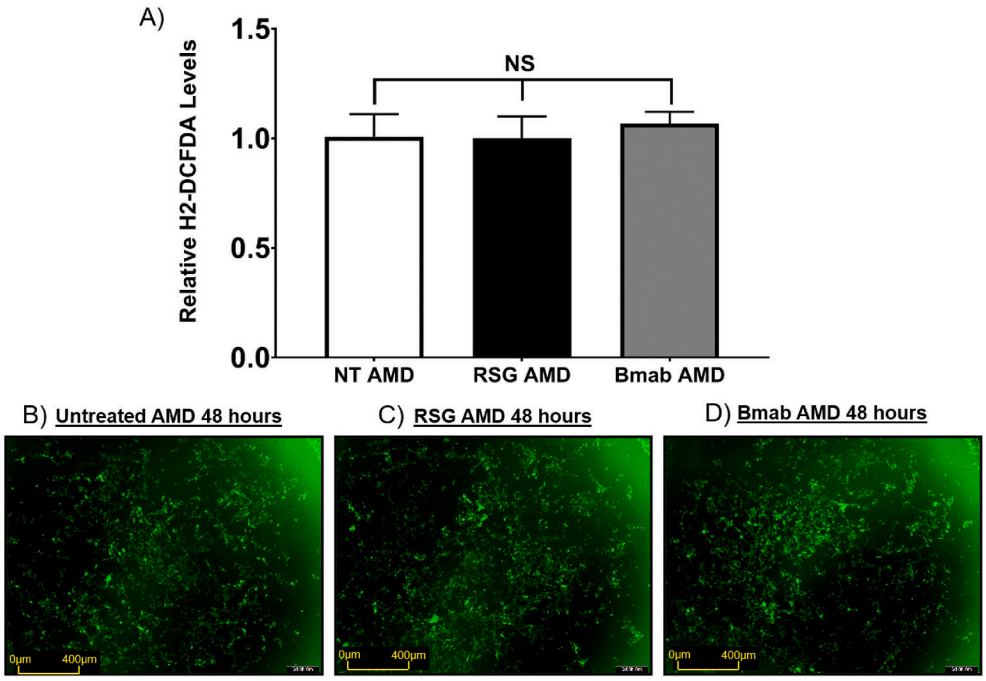

Fig. 3. RSG and Bmab had no detectable effect on ROS levels in AMD cybrids.

(A) No significant changes were seen in H2DCF-DA fluorescence levels after treatment with RSG or Bmab in AMD cybrid cells. **(B–D)** Representative H2DCF-DA fluorescence images from untreated, RSG-, and Bmab-treated AMD cybrid cells. AMD cybrids (n = 5) Data were subjected to statistical analyses by nonparametric Mann-Whitney *U* test using GraphPad Prism (Version 5.0, La Jolla, CA). A P-value of ≤0.05 was considered statistically significant (* <0.05, ** <0.01, *** <0.001, NS representative of non-significance). Error bars in the graphs represent SEM (standard error of the mean).

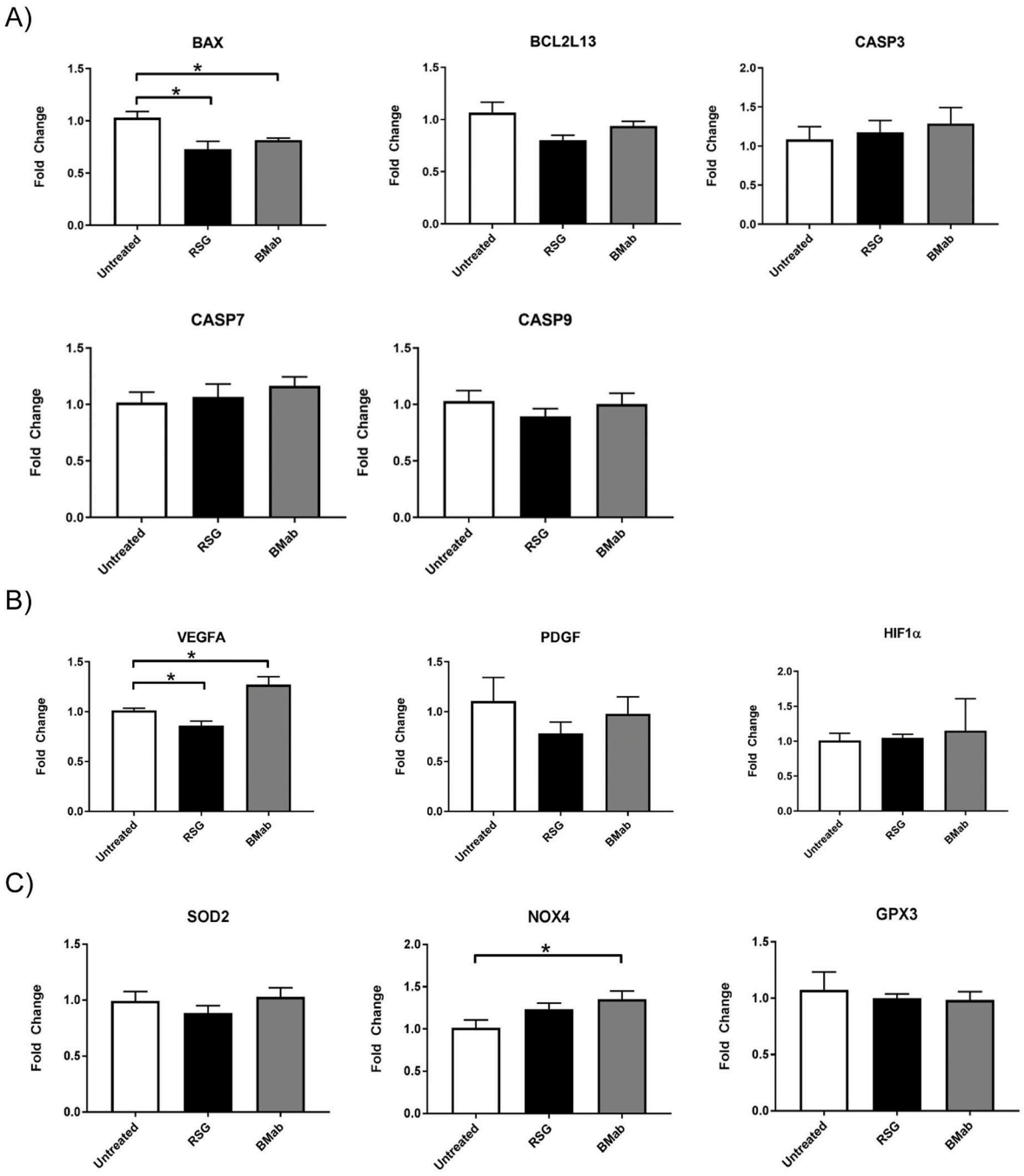

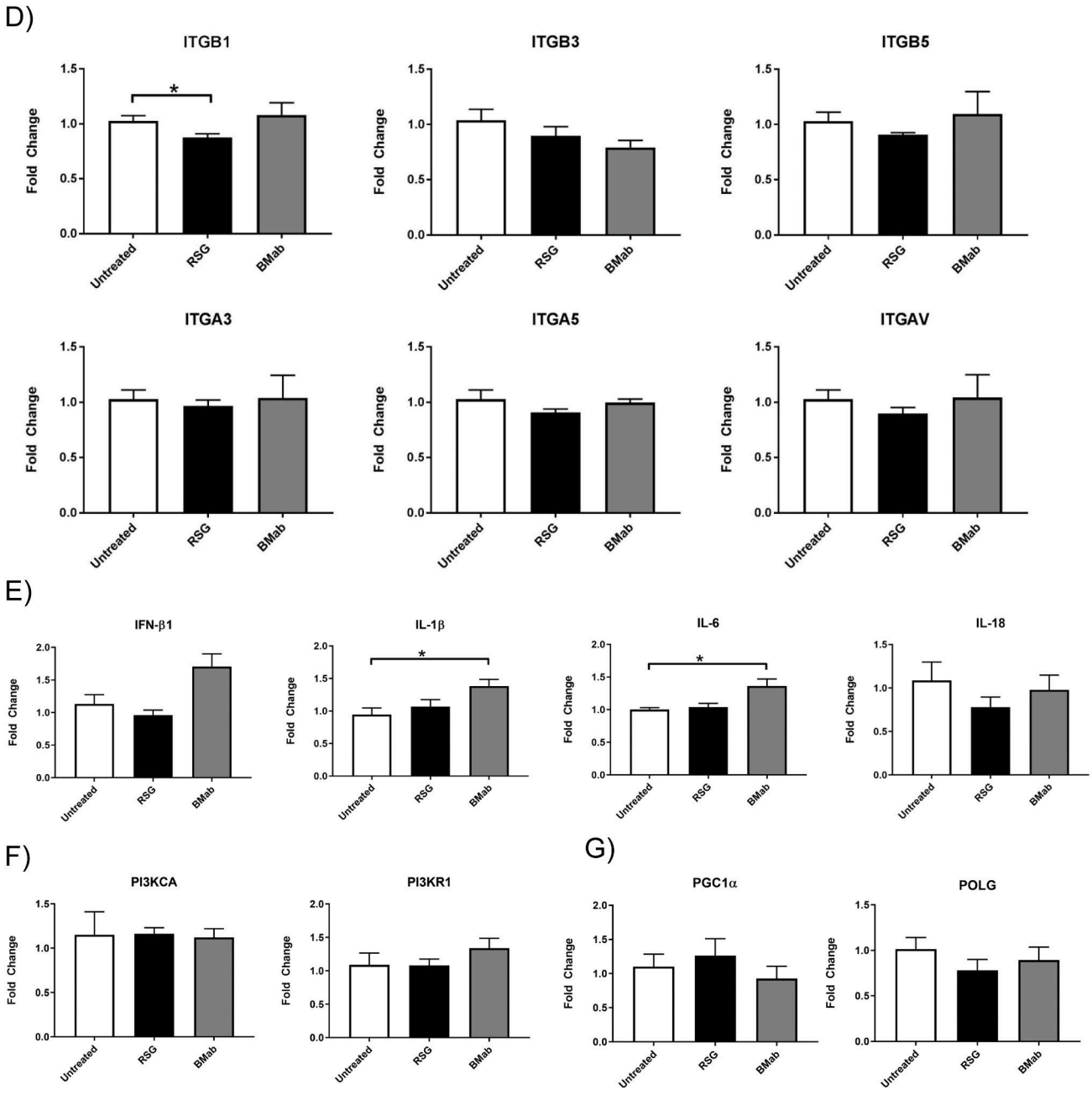

Fig. 4. RSG and Bmab treatments influenced gene expression in pathways relating to apoptosis, angiogenesis, oxidative stress and inflammation.

(A) RSG decreased expression of the pro-apoptotic genes *BAX* by 28% (0.72-fold, p = 0.0159). Treatment with Bmab decreased *BAX* gene expression by 16%. (0.84-fold, p = 0.016). Expression of CASP-3, −7, −9 were not influenced by either treatment. **(B)** RSG decreased gene expression of *VEGFA* by 20% (0.8-fold, p = 0.0357) while Bmab increased expression by 27.2% (1.272-fold, p = 0.0357); *PDGF* and *HIF1a* were not influenced by either treatment. **(C)** RSG had no effect on *SOD2*, *GPX3* or *NOX4*. Bmab increased expression of *NOX4* by 35.5% (1.355-fold, p = 0.0159) **(D)** RSG decreased expression of *ITGB1 by 13%* (0.87-fold, p = 0.0317), an integrin gene associated with angiogenesis. **(E)**

RSG treatment had no effect on expression of *IFN-β1, IL-1β, IL-6* or *IL-18*, while treatment with Bmab increased expression of *IL*-6 by *36%* (1.36-fold, p = 0.0303), and *IL-1β by 38.3%* (1.383-fold, p = 0.0381). **(F)** There was no change in either *PI3KCA* or *PI3KR1* expression under either treatment. **(G)** Finally, there was no change in *PGC1a* or *POLG*, genes associated with mitochondrial biogenesis, under either treatment. AMD cybrids (n = 5) Data were subjected to statistical analyses by nonparametric Mann-Whitney *U* test using GraphPad Prism (Version 5.0, La Jolla, CA). A P-value of ≤0.05 was considered statistically significant (* <0.05, ** <0.01, *** <0.001, NS representative of non-significance). Error bars in the graphs represent SEM (standard error of the mean).

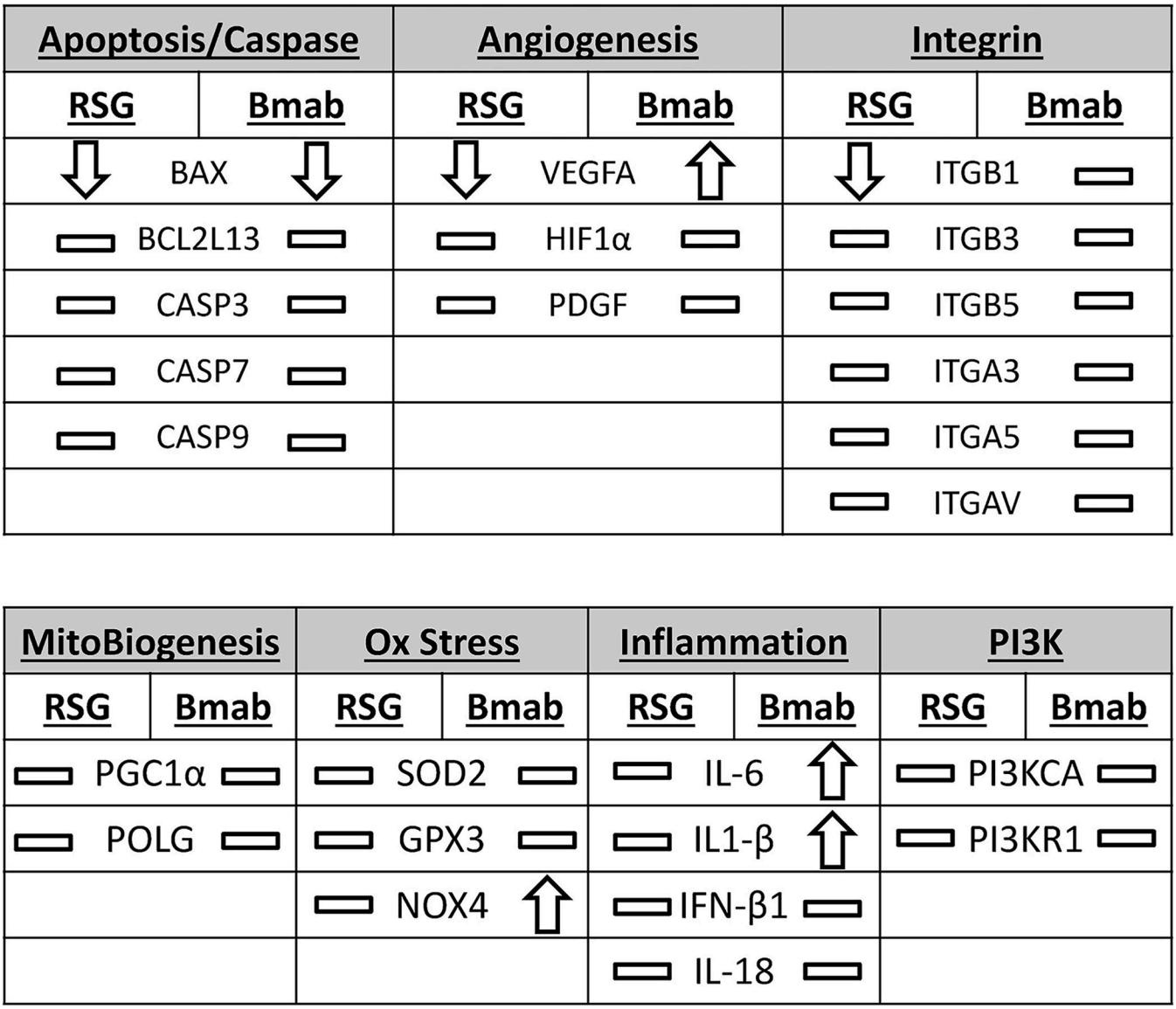

Fig. 5. Summary of the Gene Expression Patterns after Treatment with RSG and Bmab.

Bmab treatment resulted in an increase in expression of genes associated with oxidative stress, inflammation, and angiogenesis, while RSG treatment decreased genes associated with apoptosis, and angiogenesis.

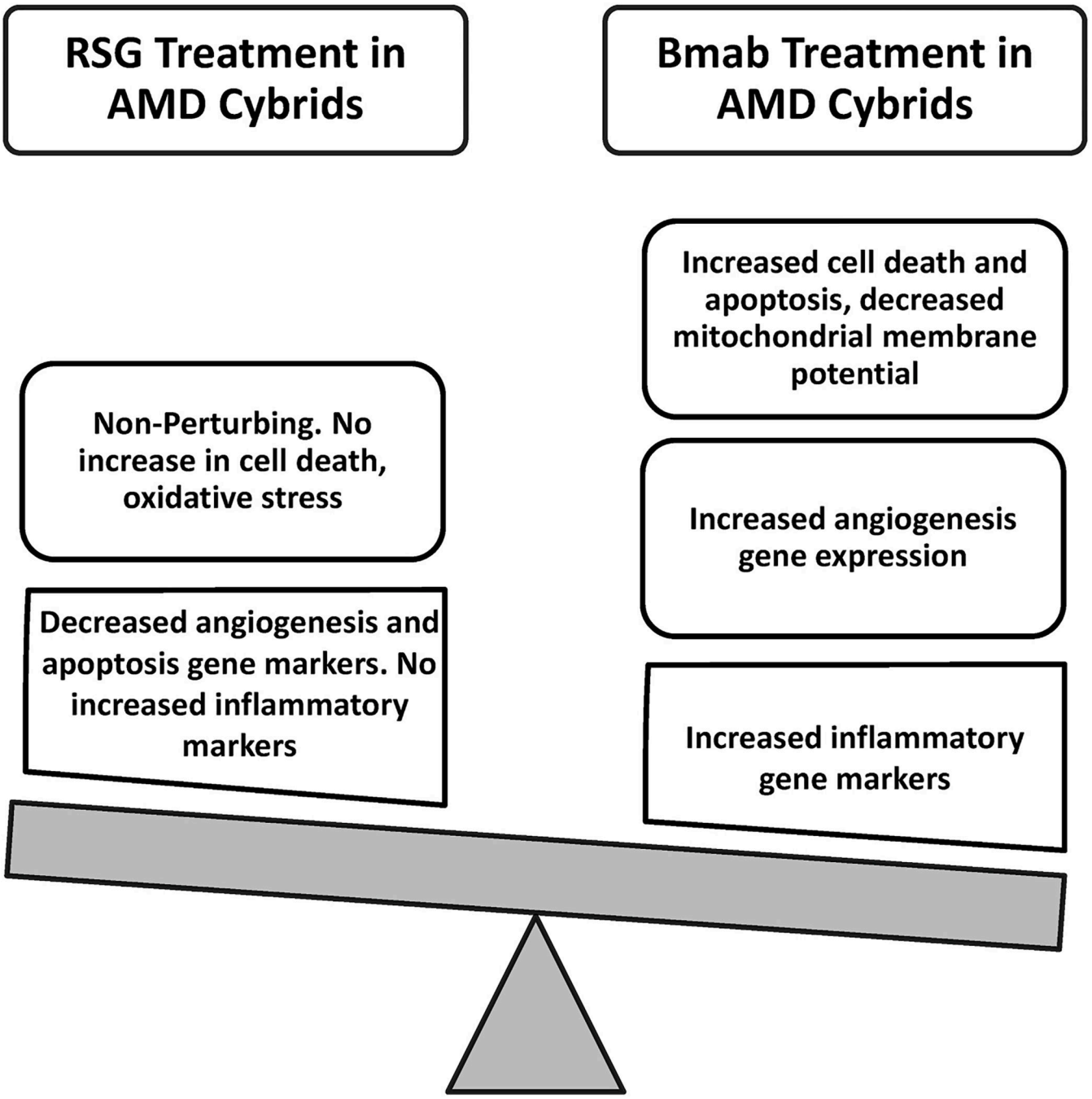

Fig. 6. Schematic Showing the Responses of AMD Cybrids to RSG versus Bmab.

Taken as a whole, results indicate that RSG is well tolerated in AMD cybrid cells, while Bmab treatment results in decreased cell health and adverse changes in gene expression.

Table 1

Demographics for subjects used to create cybrids.

Cybrid	Age	Sex	Haplogroup	Disease
AMD 14_139	81	F	H17b	Wet
AMD 14_144	86	F	H1Fa2	Wet
AMD 14_145	84	F	H7	Wet
AMD 14_146	75	F	H7c6	Wet & Dry
AMD 15_159	74	M	H11a	Wet
Cyb 14_132	78	M	H3an	Normal
Cyb 14_135	75	F	H1c3	Normal
Cyb 15_152	69	F	H1	Normal

AMD ages = 80.0 ± 2.39 (Mean ± SEM) N = 5.

Normal ages = 74.0 ± 2.645 (Mean ± SEM) N = 3.

Difference = −6.0 ± 3.724.

P = 0.1582

Table 2

Description of Genes Analyzed by qRT-PCR.

Symbol	Gene Name	Gene RefSeq Number
BAX	Bcl-2-associated X protein	NM_001291428
		NM_001291429
		NM_001291430
		NM_001291431
		NM_004324
BCL2L13	BCL2-like 13 (apoptosis facilitator)	NM_001270726
		NM_001270727
		NM_001270728
		NM_001270729
		NM_001270730
CASP3	Caspase-3	NM_004346
		NM_032991
CASP7	Caspase-7, apoptosis-related cysteine peptidase	NM_001227
		NM_001267056
		NM_001267057
		NM_001267058
		NM_033338
CASP9	Caspase-9	NM_001229
		NM_001278054
		NM_032996
VEGFA	Vascular endothelial growth factor A	NM_003376
		NM_001025366
		NM_001025367
		NM_001025368
		NM_001025369
HIF1α	Hypoxia-inducible factor 1-alpha	NM_181054
		NM_001243084
		NM_001530
PDGF	Platelet-derived growth factor	NM_033016
		NM_002608
ITGB1	Integrin beta-1	NM_002211
		NM_033666
		NM_033667
		NM_033668
		NM_033669
ITGB3	Integrin beta-3	NM_000212
ITGB5	Integrin beta-5	NM_002213
		NM_001354764
		NM_001354765

Symbol	Gene Name	Gene RefSeq Number
		NM_001354766
ITGA3	Integrin alpha-3	NM_002204
		NM_005501
ITGA5	Integrin alpha-5	NM_002205
ITGAV	Integrin alpha-V	NM_001144999
		NM_001145000
		NM_002210
PGC1α	Peroxisome proliferator-activated receptor gamma coactivator 1-alpha	NM_013261
		NM_001330751
		NM_001330752
		NM_001330753
POLG	DNA polymerase subunit gamma	NM_002693
		NM_001126131
SOD2	Superoxide dismutase 2	NM_000636
		NM_001024465
		NM_001024466
		NM_001322814
		NM_001322815
GPX3	Glutathione peroxidase 3	NM_002084
		NM_001329790
NOX4	NADPH oxidase 4	NM_001143836
		NM_001143837
		NM_001291926
		NM_001291927
		NM_001291929
IL-6	Interleukin 6	NM_000600
		NM_001318095
		NM_001371096
IL-1β	Interleukin 1 beta	NM_000576
IFN- β1	Interferon type I beta	NM_002176
IL-18	Interleukin 18	NM_001243211
		NM_001562
PI3KCA	Phosphatidylinositol-4,5-bisphosphate 3-kinase, catalytic subunit alpha	NM_006218
PI3KR1	Phosphatidylinositol 3-kinase regulatory subunit alpha	NM_001242466
		NM_181504
		NM_181523
		NM_181524
		HOUSEKEEPERS
HPRT1	Hypoxanthine phosphoribosyltransferase 1	NM_000194
HMBS	Hydroxymethylbilane synthase	NM_000190; NM_001024382
		NM_001258208; NM_001258209